Applications of AVHRR-Derived Ice Motions for the Arctic and Antarctic

NAG 5-4119
NAGW-4402 (Previous Year's Grant Number)

Final Report

NASA
Polar Oceans Branch
Dr. P. Gogineni, Program Manager
NASA Headquarters
Washington, DC 20543

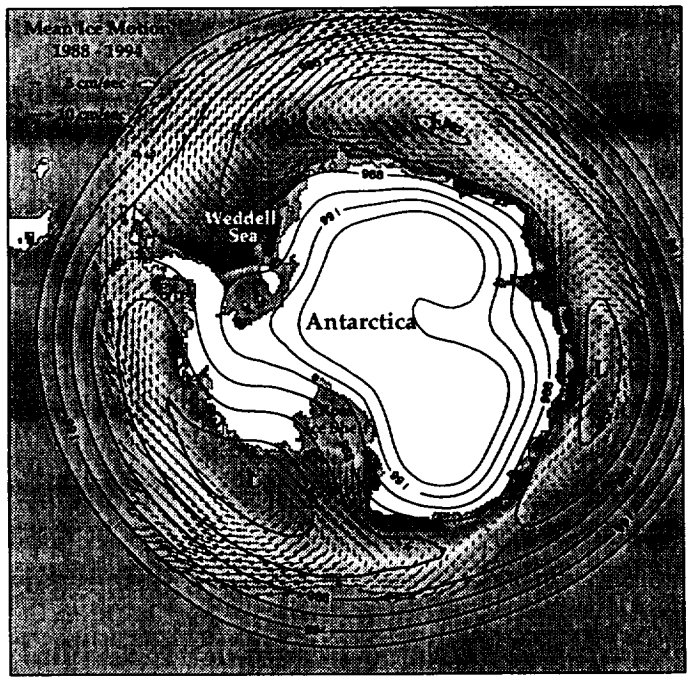

Principal Investigators:

James Maslanik
CCAR, CB431
University of Colorado
Boulder, Colorado 80309
ph. 303-492-8974
fax 303-492-2825
jimm@northwind.colorado.edu

William Emery
CCAR, CB431
University of Colorado
Boulder, Colorado 80309
ph. 303-492-8591
fax 303-492-2825
emery@frodo.colorado.edu

1.0 Summary

Characterization and diagnosis of sea ice/atmosphere/ocean interactions require a synthesis of observations and modeling to identify the key mechanisms controlling the ice/climate system. In this project, we combined product generation, observational analyses, and modeling to define and interpret variability in ice motion in conjunction with thermodynamic factors such as surface temperature and albedo. The goals of ths work were twofold: (1) to develop and test procedures to produce an integrated set of polar products from remotely-sensed and supporting data; and (2) to apply these data to understand processes at work in controlling sea ice distribution.

Main tasks during the project include:

- Development and testing of methods to retrieve improved ice motion data from satellite imagery, including extension to SMMR and SSM/I passive microwave data;
- Testing of methods to combine ice motion data from different sources, including statistical optimal interpolation and use of a 2-dimensional sea ice model as an interpolator in data assimilation mode;
- Applications of remotely-sensed ice motions to document spatial and temporal patterns of ice transport;
- Identification and diagnosis of the role of ice transport in the record Arctic sea-ice extent anomaly of 1990;
- Documentation of the significance of ice transport variations as a function of sea level pressure indices;
- Examination of the role of large-scale ice transport in affecting simulations of climate change ;
- Applications of remotely-sensed ice motion data to evaluate the performance of sea-ice and climate models;

Key findings from these tasks include:

- Ice motion data retrieved from passive microwave data (85, 37, and 19 GHz channels) provide previously unseen levels of detail for the Arctic and Antarctic over a time span equivalent to that of drifting buoys;
- A revised MCC method including relaxation techniques offers the potential to yield improved ice motion fields;
- Combining remotely-sensed ice motions with a 2-D dynamic-thermodynamic ice model offers potential for model improvement as well as for use of the model as a physically-based interpolator;
- Ice extent anomalies, and the simulated responses of the sea ice pack to climate perturbations, are strongly linked to ice transport patterns;

- Ice motion data, ice concentrations, sea level pressures, and simulated ice conditions suggest two distinct modes of Arctic ice transport linked to positive and negative NAO patterns. The data reflect a persistent positive NAO pattern seen during 1979 through the mid-1990's;
- The remotely-sensed ice motion grids lend themselves well for use as model evaluation data sets, but since these data represent years of abnormal Arctic sea level pressure patterns, care must be taken when comparing model output to long-term mean motion patterns;

Thirteen publications were supported fully or in part by this grant. An additional 3 manuscripts are in preparation or have been submitted for publication. The supported publications are indicated by an asterisk in the references in Section 4.

The following sections provide additional details for each of these major topics.

2.0 Results

2.1 Retrieval of Ice Motion Data from Satellite Imagery

The original proposal addressed the applications of the maximum cross-correlation (MCC) method to extract ice displacement information from Advanced Very High Resolution Radiometer (AVHRR) imagery. This work continued during the grant period, but was augmented by taking advantage of newly published results where displacements were calculated from Special Sensor Microwave/Imager (SSM/I) data (Agnew et al., 1996; Liu et al., 1998). Building upon these earlier works, we adapted our existing MCC routines to accomodate 85 GHz SSM/I data. Optimal interpolation procedures used to blend AVHRR and drifting buoy data as part of the AVHRR-based Polar Pathfinder were applied to merge the SSM/I data with buoys.

The ice motion retrieval procedure was then extended to include testing of 37 GHz data. This lower-frequency channel has the advantage of less sensitivity to atmospheric effects and consistency between the Scanning Multichannel Microwave Radiometer (SMMR) and SSM/I, which allows a longer time series of ice motion. The primary disadvantage is the lower spatial resolution at 37 GHz, which degrades the accuracy of the retrieved ice motion data. Applications to SMMR and SSM/I data has allowed us to generate a uniform grid of ice motions for the Arctic and Antarctic for 1979-1997. Figures 1 and 2 illustrates some of the different characteristics of velocities calculated using 37 GHz and 85 GHz data. Both channels capture the same basic patterns in these monthly means, but note the additional detail apparent in the 85 GHz data for the Arctic. On the other hand, in the Antarctic example, atmospheric effects

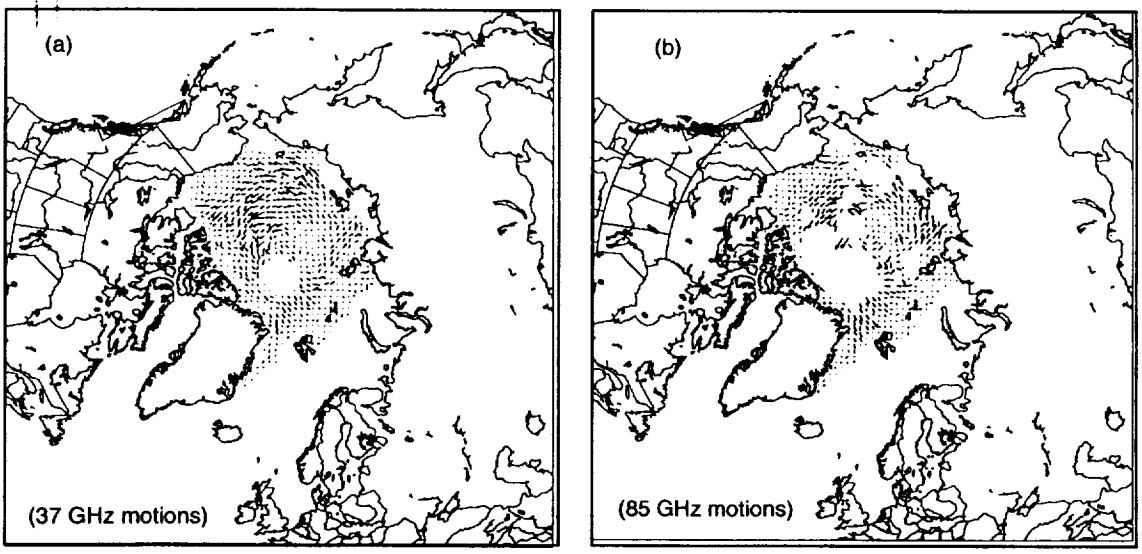

Figure 1. Comparison of Arctic ice motion derived from 37 GHz (a) and 85 GHz (b) data for September 1988.

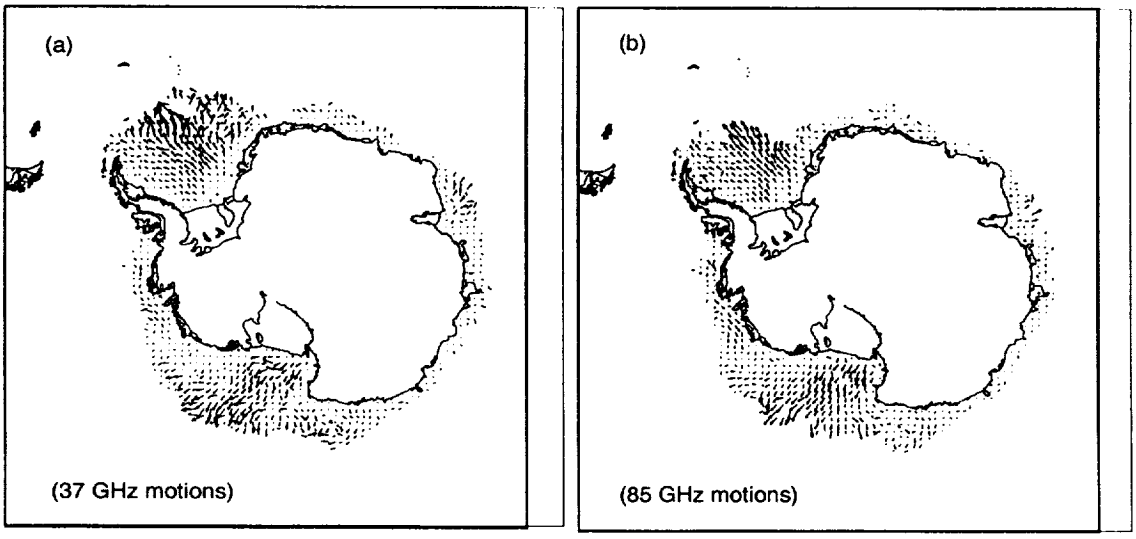

Figure 2. Comparison of Antarctic ice motion derived from 37 GHz (a) and 85 GHz (b) data for April 1996.

obscure a portion of the Weddell Sea ice motion pattern in the 85 GHz data, but the additional area is revealed in the 37 GHz data

We find that the obscuration of the SMMR and SSM/I data is particularly significant in the Antarctic. As with AVHRR data, the potential exists to introduce biases into long-term mean motion fields if the ability to map ice motions is affected substantially by atmospheric conditions. We have therefore tested an enhancement to the MCC method that offers the potential for useful motion data retrievals from the SMMR 18 GHz and SSM/I 19 GHz channels.

Most efforts to extract ice motion data from satellite imagery have relied on some form of the maximum cross-correlation method (MCC). Alternative methods such as wavelet analysis typically carry significant penalties for operational use. In the MCC approach, a small sub-section of an image (template) is cross-correlated with same-size areas in a second image. The location that produces the largest correlation coefficient is considered the displacement of the ice over the time between the image pair. The "actual" displacement, however, may not be found because of several causes. These factors can all be considered noise and may be from atmospheric effects, changes in the ice emissivities, non-linear distortions of the surface area, etc. Therefore, the maximum correlation location may not correspond to the "correct" location.

Current computation of ice velocities by most researchers is at least a two step process. First, the ice displacements are computed using the MCC method. Then a post-processing filtering is applied to remove obviously "bad" vectors. The filtering is based on the assumption that small areas of ice do not move independently of neighboring areas of ice. By comparing an ice vector with near-by vectors, some vectors can be removed.

An alternative approach that extends the MCC method is a relaxation-labeling technique (Rosenfeld and Kak, 1982; Wu, 1995). Essentially, the relaxation-labeling combines the MCC method with the filtering assumptions to select a "better" vector, and hence removes most of the requirement for filtering as a second step. Relaxation-labeling is implemented in much the same manner as the original MCC method, but instead of selecting the displacement with the maximun correlation, an iterative approach is taken in selecting the correct vector. Because of noise, the correlation values may have more than one peak, or the surface may have a flattened appearance. All correlation coefficients above a prescribed cut-off are chosen. Each value is evaluated with all chosen values from neighboring locations. Each value is then weighted based on how similar it is to the other values. Therefore, a value with more support increases, and decreases the more dissimilar it is with near-by values. This process is repeated until the total change of all values from the previous iteration is less than a chosen threshold. As a

result, a more coherent ice flow field is produced, and little or no post-filtering is needed.

Figures 3a and 3b show the level of improvement that appears possible using this new method versus our standard method. The motion field in Fig. 3a includes no post-processing filtering, is more complete and spatially consistent than the MCC results, and also shows additional detail not seen in the MCC output in Fig. 3b. Tests suggest that relatively little detail in spatial patterns are lost using the lower-frequency data, but the effects of atmospheric moisture and possibly surface melt are reduced.

These improvements in the original MCC approach appears to work well for the lower-frequency SMMR and SSM/I data. Extension to these lower frequencies has allowed us to consider the possible use of Electronically Scanning Microwave Radiometer (ESMR) imagery to extend the possible record of motion data to include 1973-1976. We have obtained ESMR brightness temperatures mapped to the SSM/I grid from GSFC in "uncorrected" and "corrected" form. Tests using the uncorrected data yielded poor results due to spurious variability in brightness temperatures. These problems are lessened in the corrected data, but substantial misregistration errors have so far precluded extraction of useful ice motion from the ESMR imagery. The ESMR data still may prove useful, but additional manual correction of the geolocation problem would be required.

During the past year, we have collaborated with Dr. Mark Drinkwater of JPL to better assess the utility of the AVHRR and passive microwave ice motion data for Antarctic applications. Preliminary results suggest that more substantial inertial motion under the Antarctic near free-drift conditions yields greater variations in the remotely-sensed data compared to drifting buoys, consistent with Dr. Drinkwater's earlier work analyzing SAR-derived ice velocities. Further, the effects of weather and melt, which limit the retrievals of the AVHRR and passive microwave-derived ice motion, appear more prevalent in the Antarctic. Some of these issues will continue to be explored as part of other NASA funding for Polar Pathfinder product validation.

2.2 Blending of Motion Data using Statistical Methods and Data Assimilation

While we have found the motion data from individual sensors to be useful for case studies, many other applications require uniformly-gridded data with few gaps in time. An objective of our work was to test improved methods of combining ice motion data from different sources. Each of the available and potentially available data sets have different temporal and spatial sampling characteristics as well as different accuracies. Our initial work has made use of statistical optimal interpolation to combine ice displacements from AVHRR, passive microwave, and buoys (e.g., Meier et al., 1997). We

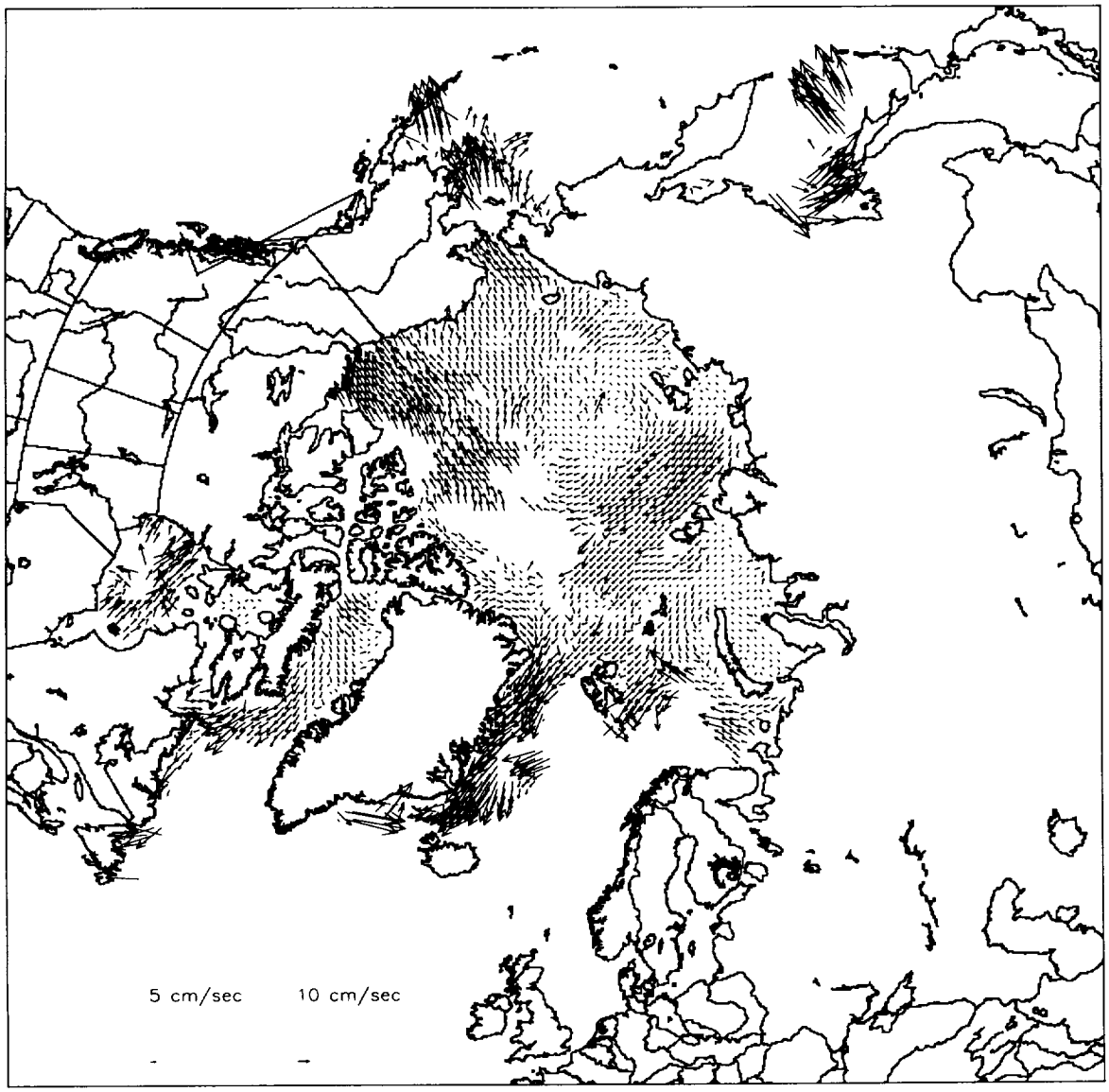

Figure3a. Ice Velocity from SSM/I 85Ghz using the MCC method with relaxation-labeling, and no post-filtering done. (March 31, 1997)

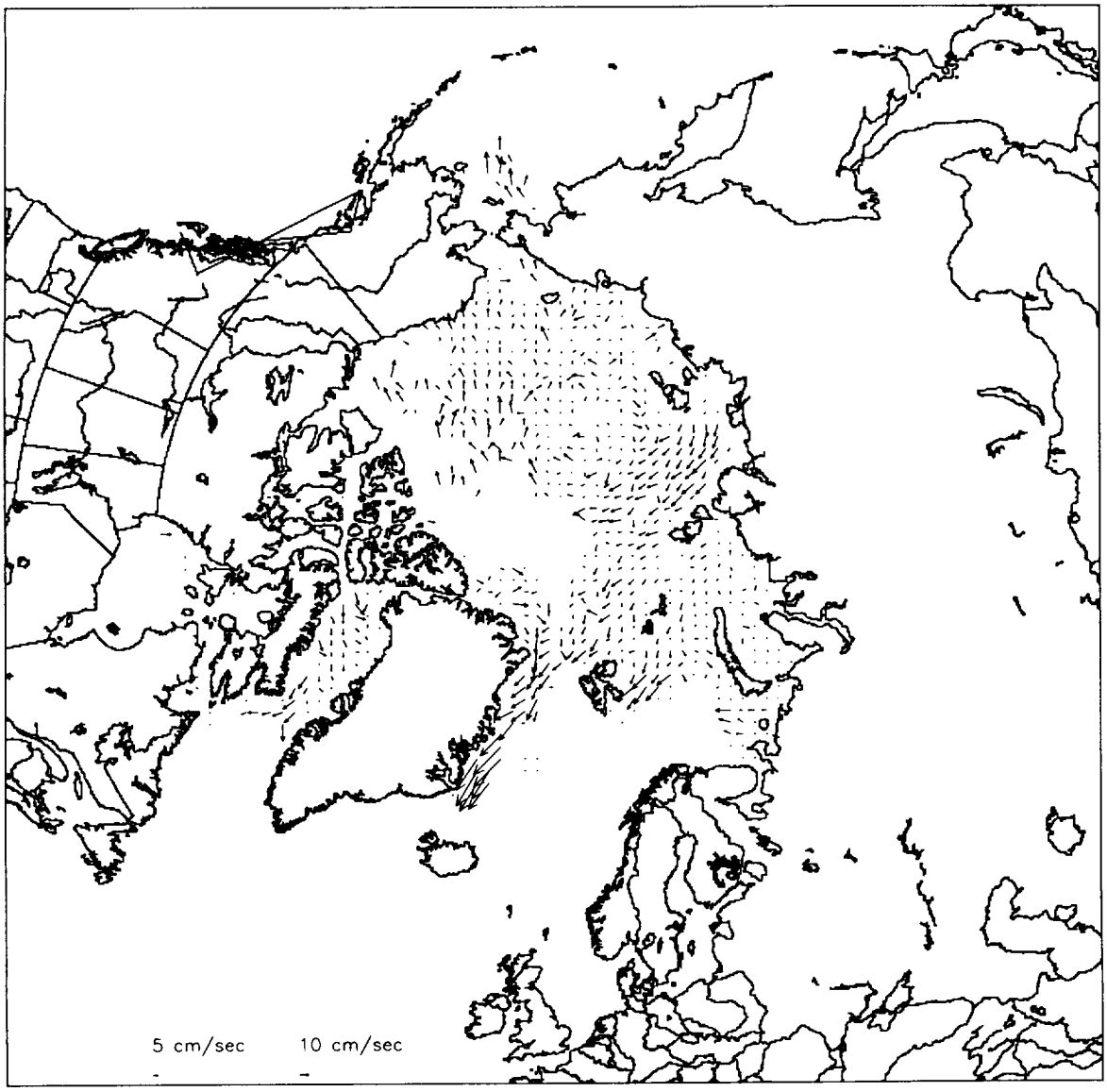

Figure3b. Same as figure 3a but using the MCC method alone with post-filtering of the vectors.

currently use this approach for generating the Polar Pathfinder products. However, the statistical interpolation has significant shortcomings in certain cases. For example, optimal interpolation is poorly suited for locations where the motion field varies strongly over short distances. We have found the approach to present particular problems in the Antarctic, where the motion field is dominated by strong and persistent gyre patterns. Also, features such as the Palmer Peninsula that affect ice drift introduce abrupt spatial variations that are not dealt with easily using standard interpolation.

To address this, we have tested several modifications to the optimal interpolation, such as including anisotropy in the weighting field. A more promising approach is the potential use of a two-dimensional ice model in data assimilation mode . In contrast to the usual goal of data assimilation to improve model predictions, we are considering the model as an interpolation tool that provides physical constraints to the interpolation. Since the model generates it's own ice velocities as a function of winds and ice rheology, this assimilation approach also has the advantage of providing a logical and defensible way of interpolating over time to fill gaps when satellite-derived motions may not be available (particularly during summer).

In our work (supported through this grant and through a NASA graduate research fellowship to Walter Meier), we have tested simple assimilation schemes using a 4-category ice model with viscous-plastic ice rheology. Methods tested include a simple weighting scheme to combine SSM/I motions with the modeled velocities. This has been extended to include an assimilation where error statistics estimated for the model alone and for the SSM/I data are used in a blending method. Overall, the mean error of the model and the SSM/I data vs. drifting buoys are comparable, such that the assimilation using this current approach yields relatively slight mean changes in the resulting simulated ice conditions for the period examined (1988-1992). The assimilation does, though, introduce a slight correction into the modeled mean motion field (Figure 4). In this example, the assimilation tends to modify the large-scale circulation in the central Arctic and add more ice transport into Fram Strait from the northern Greenland Sea. For individual days, where the observed and modeled motion field can differ substantially, the assimilation brings the resulting blended motion field more in line with actual conditions.

Our assimilation work to date has pointed out a number of questions that will require additional research. For example, depending on whether the goal is to improve the sea ice model or to use the model as a data interpolator in space and time, different assimilation strategies may be appropriate. In our current approach, a conservative path is taken to avoid introducing large inconsistencies into the model, such as a suppression of deformation that occurs over short periods. In this particular case, since the ice motion data we use are obtained from daily-averaged brightness temperature grids, the time

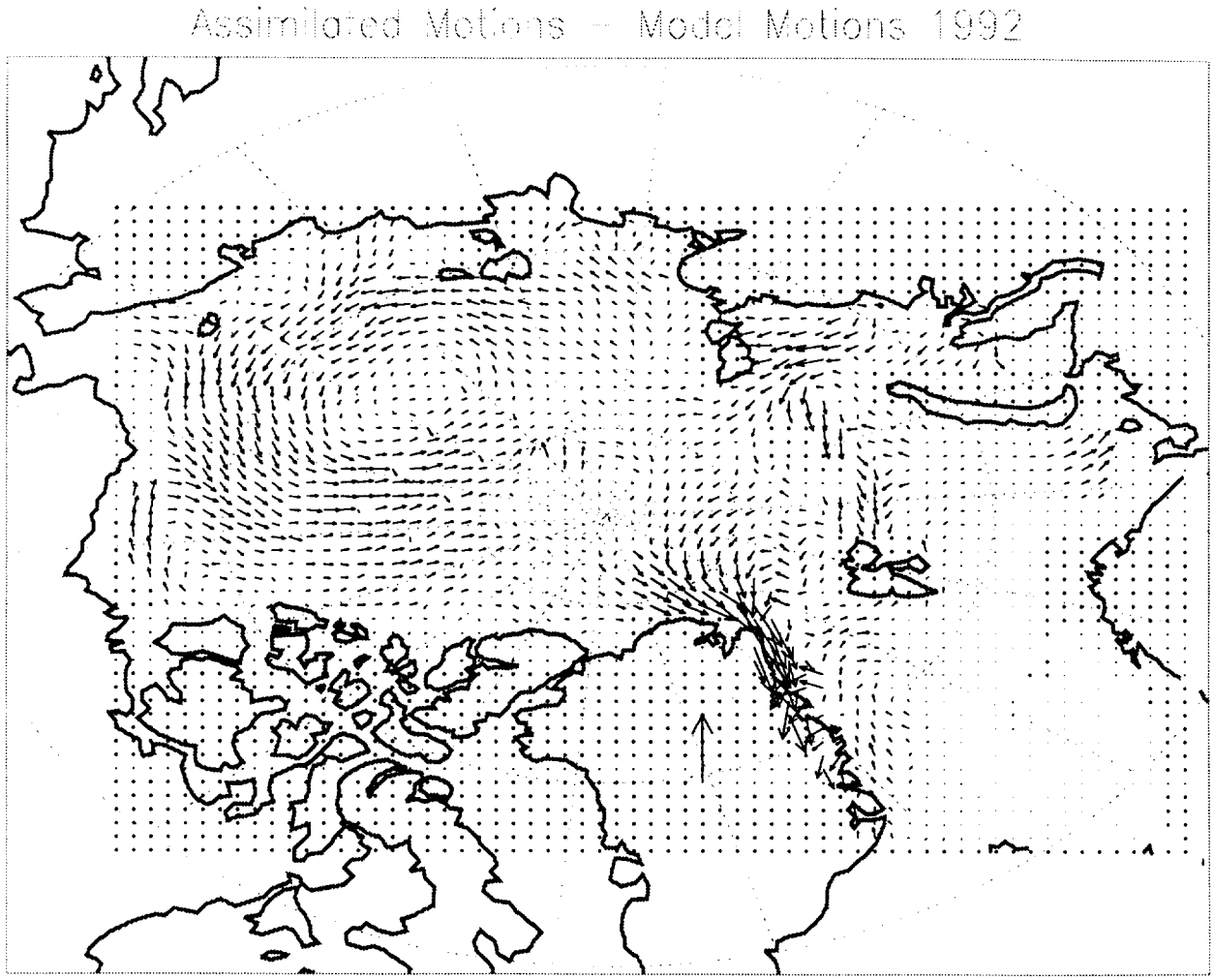

Figure 4. The effects on mean motion fields of assimilating SSM/I-derived ice velocities within a 2-D ice model for 1992. The vectors show the total difference in ice velocity due to assimilating the remotely-sensed ice motion data.

sampling of the SSM/I-derived motions is less than that of the model time step (8-hourly in our model runs). In the future, model time steps and the availability of wind fields to force the model at those steps will become increasingly detailed. However, there is little hope of obtaining remotely-sensed ice motion data at finer than daily intervals. Thus, our assimilation work is pointing out potential inconsistencies between existing data sets versus the characteristics that are optimum for assimilations. In many instances, the polar community faces different problems than have been addressed by the atmospheric modeling community, which is the source of much of the data assimilation literature and methods.

Future research will need to consider issues such as: (1) how best to incorporate data to avoid smoothing of short-period variations while minimizing biases over longer time scales; (2) how to ingest a range of data types that have substantially different time sampling and spatial resolution (such as SAR data, buoys, and SSM/I) but that pertain to an individual variable such as ice motion; and (3) whether other variables such as ice concentration or snow conditions might best be dealt with using a forward modeling approach that is based on comparisons of simulated and observed radiances rather than assimilation of geophysical products - the characteristics of which can be quite different depending on the sensor and algorithm used to generate the data set. An example is ice concentration, which will differ more or less depending on the data source and which also may be significantly different from the definition of "ice concentration" within the ice model. For example, a typical two-category ice model considers ice concentration to consist only of thick ice, while all area of thickness less than some value (typically 0.5 m) is considered as "thin ice/open water". Such differences in definition are critical to the assimilation, and must be fully understood by the data producer as well as by the modeler using data.

2.3 Applications of Ice Motion Data to Document Large-Scale Transport Patterns

A seven-year time series of interpolated and SSM/I-only motions was used to provide a uniquely comprehensive view of ice motion for the Arctic and the Antarctic, including areas for which little or no previous ice motion data have been readily available (Emery et al., 1997). For example, Figure 5 shows the remotely-sensed ice motion mean field for the Southern Ocean. In the Antarctic, for example, means calculated from daily ice displacements for 1988-1994 confirm the basic circulation patterns established from drifting stations and buoys, but extend these observations to illustrate less well-known transport patterns in the Arctic coastal zones and sub-Arctic seas. In the Antarctic, the gridded motion fields show a nearly continuous westward transport along the Antarctic coast, with well-defined regions of exchange between this East Wind Drift and the Antarctic Circumpolar Current.

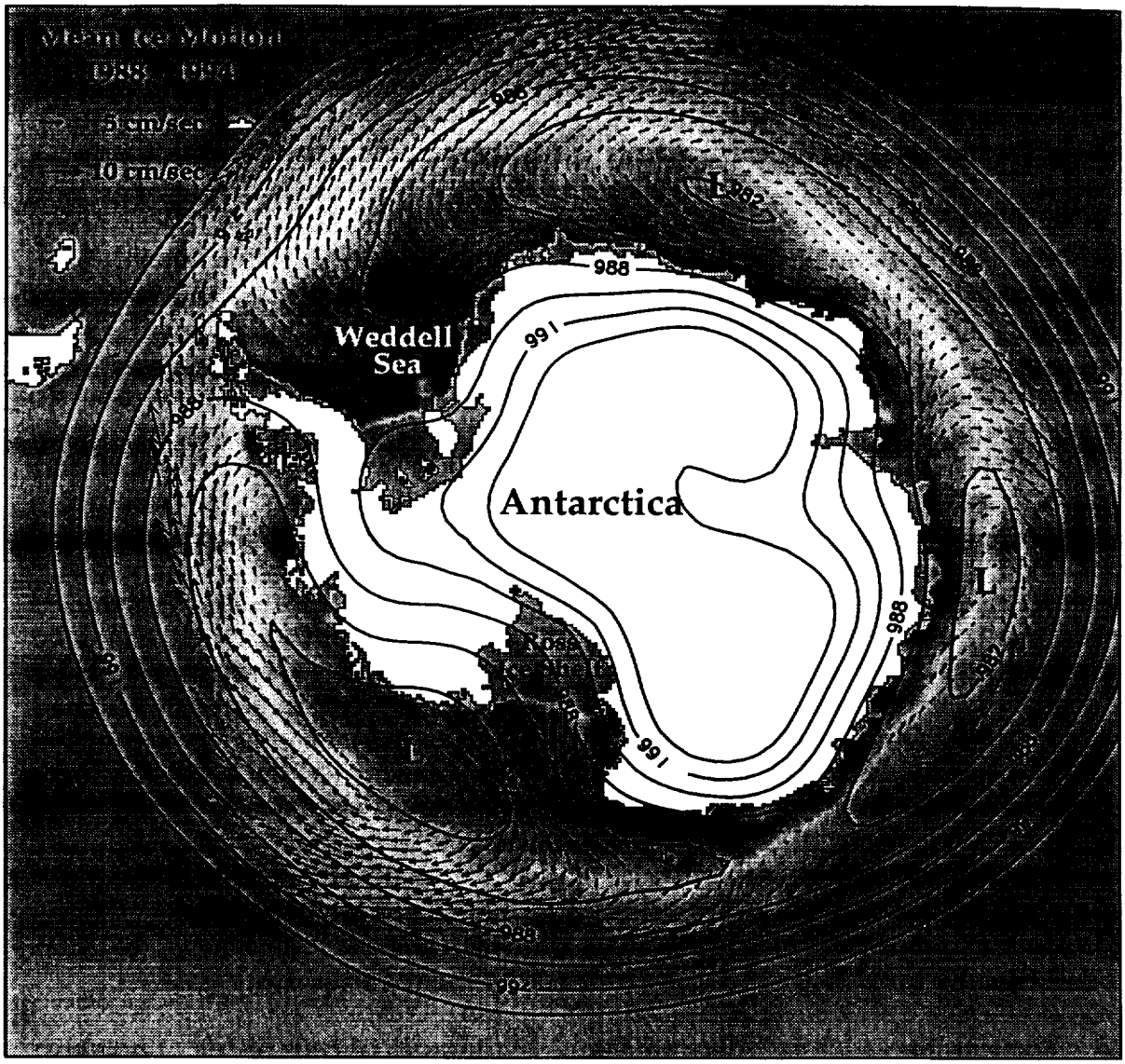

Figure 5 Satellite-derived mean sea-ice velocities and ice concentration for 1988 - 1994. Superimposed on the ice velocity vectors are contours of mean sea level pressure for the same period. Note the correspondence between ice drift patterns and the locations of low pressure systems ("L"). These time series are now being produced operationally as part of the Polar Pathfinder project.

In addition to providing a basic overview of ice conditions, the remotely-sensed motion fields have been used to investigate seasonal variations and details of regional ice transport. An example of possible applications include the study of potential routes of pollutant transport. Using the ice motion data, trajectories of pollutants were calculated to simulate mean transport routes and the likely dispersal of pollutants over time (Emery et al., 1998). Three-year displacements of contaminants from a number of Russian sites and one American site display various behaviors from substantial displacement and dispersal to almost no movement. As illustrated in Figure 6, the dispersion can be seasonally dependent and can vary substantially depending on the precise location where the contaminant is deposited.

2.4 Investigations of Climate-Scale Interactions of Ice Motion, Ice Extent, and Atmospheric Forcings

2.4.1 The Nature and Role of Regional Variations

Hemispheric averages of sea ice extent (ocean area with at least 15% ice) suggest a general downward trend in ice cover for 1979-1996, as mapped using passive microwave satellite imagery. In the Arctic Ocean proper, the sea-ice trend is dominated by relatively large reductions in summer ice extent as well as increased variability in recent years (Figure 7). For example, the largest negative and positive anomalies in summer ice extent in the Arctic Ocean have occurred since 1989. As suggested by the patterns in Figure 8, much of this variability is related to changes in ice cover in the Siberian and Barents sectors of the Arctic.

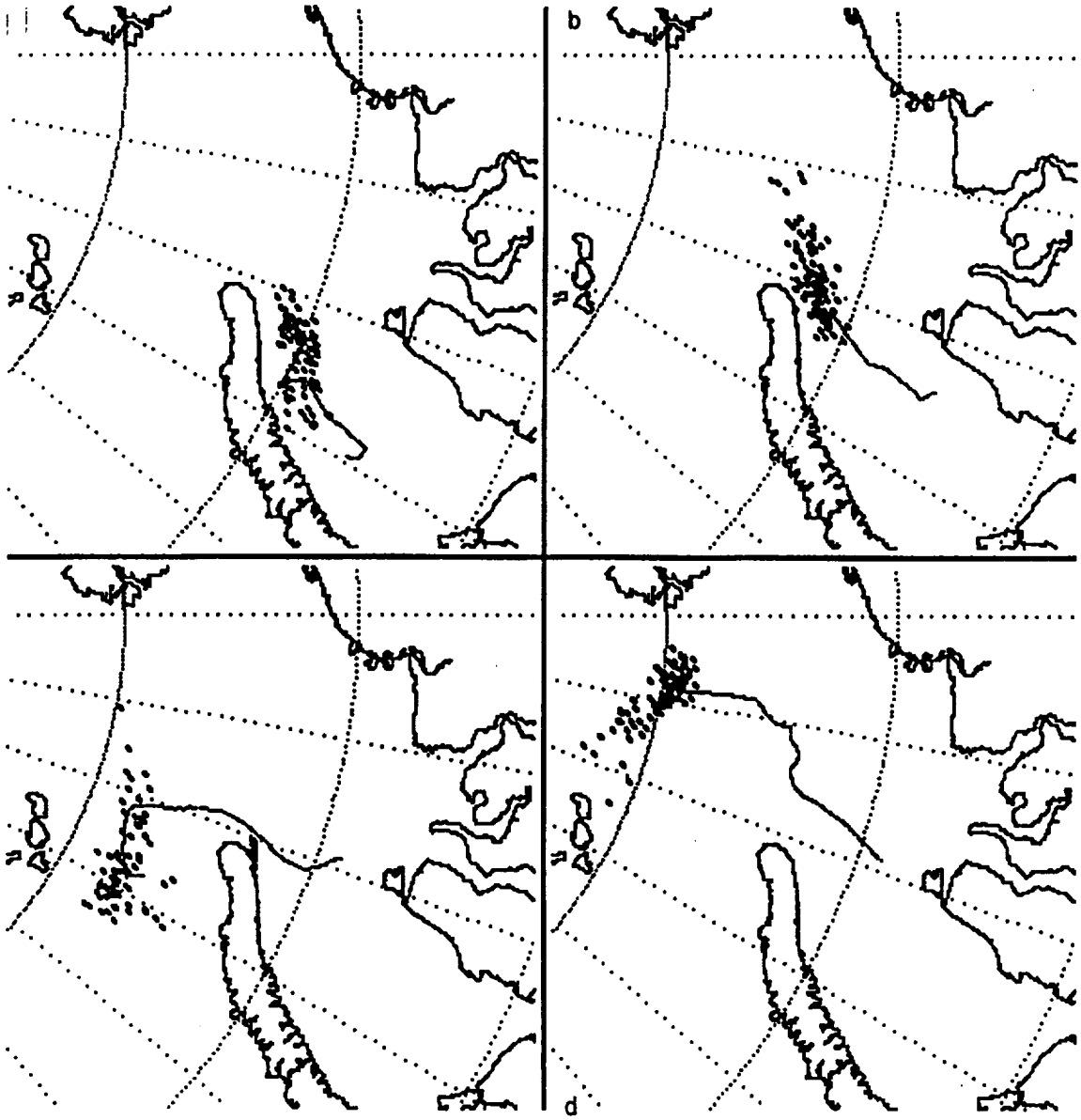

Figure 6. Advection and dispersion of a contaminant deposited in the southern central Kara Sea. The top two panels compare drift and dispersion for contaminants deposited at different locations in September. The bottom panels compare drift for deposition in September (left) and February (right).

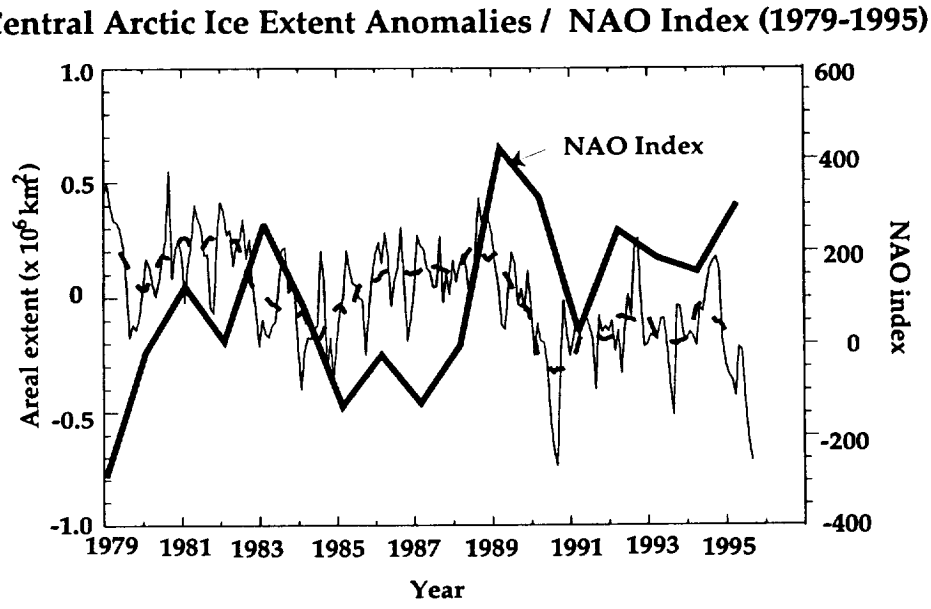

Figure 7. Anomalies of Arctic Ocean ice extent for 1979-1996. Also shown is the corresponding index of the North Atlantic Oscillation (NAO).

Figure 8. Trends in Northern Hemisphere ice concentration for 1979-1995. (Increasing ice = white; decreasing ice = dark gray). Data obtained from the National Snow and Ice Data Center.

The regional nature of the sea ice trends in Figure 8 indicate linkages to synoptic-scale atmospheric circulation rather than to a global increase in air temperatures, and are consistent with trends in other climate observations. If global warming manifests itself as an increase in the frequency or intensity of preferred atmospheric circulation patterns rather than as a linear response to air temperatures, then accurate simulation of the global-warming response requires that regional structure be correctly modeled. Climate-change predictions thus will depend in part on the ability of climate models to reproduce the observed range of regional variability. Newer GCMs include dynamical-thermodynamical ice models, but this addition of ice transport may be of minimal value, and perhaps even make matters worse, if the GCMs do a poor job of simulating the winds and ocean currents that move ice to where it ought to be.

Since the ice pack is controlled by interactions among ice transport and ice growth/melt, such regional patterns provide a useful target for investigations using ice motion data. In particular, the reductions in ice extent in the Siberian Arctic seen in Figure 8 are related in part to an increase in cyclonic activity over the Arctic Ocean since 1989, which has occurred in conjunction with, or perhaps as a modification of, the positive mode of the North Atlantic Oscillation that has persisted in recent years. The resulting wind patterns bring warm air into the Arctic Ocean and advect ice away from the Eurasian coastal areas. Since air temperatures over the Siberian continent have increased over time, these weather patterns act to link the Arctic Ocean to the observed continental warming.

To investigate further the interactions between large-scale ice transport, atmospheric circulation, and trends in ice cover, ice-model simulations for were carried out using NCEP forcings for 1985-1993. The simulations suggest that after mid-1988, total ice thickness in the Arctic Ocean may have decreased in conjunction with the observed ice and atmosphere trends (Figure 9). This decrease occurs mostly in the Eurasian sector with some increase in the western Arctic, as suggested by observed changes in ice conditions and ice transport. For example, operational ice forecasters have noted a decrease in old, thick ice in the Eurasian Arctic in the early 1990's. Such a decrease is consistent with the observed ice transport patterns, and agrees with the ice model's estimate of ice thickness and age. The greater variability of the observed ice extent is also consistent with a thinner ice pack, which can respond more readily to changes in air temperatures or wind direction. Also consistent with this are apparent reductions in ice fraction in the central Arctic in summer 1996. The magnitude of these reductions in 1996 and the physical appearance of the pack ice are more typical of regions covered by seasonal ice cover rather than the perennial, thick, high-concentration ice pack typical of the interior Arctic.

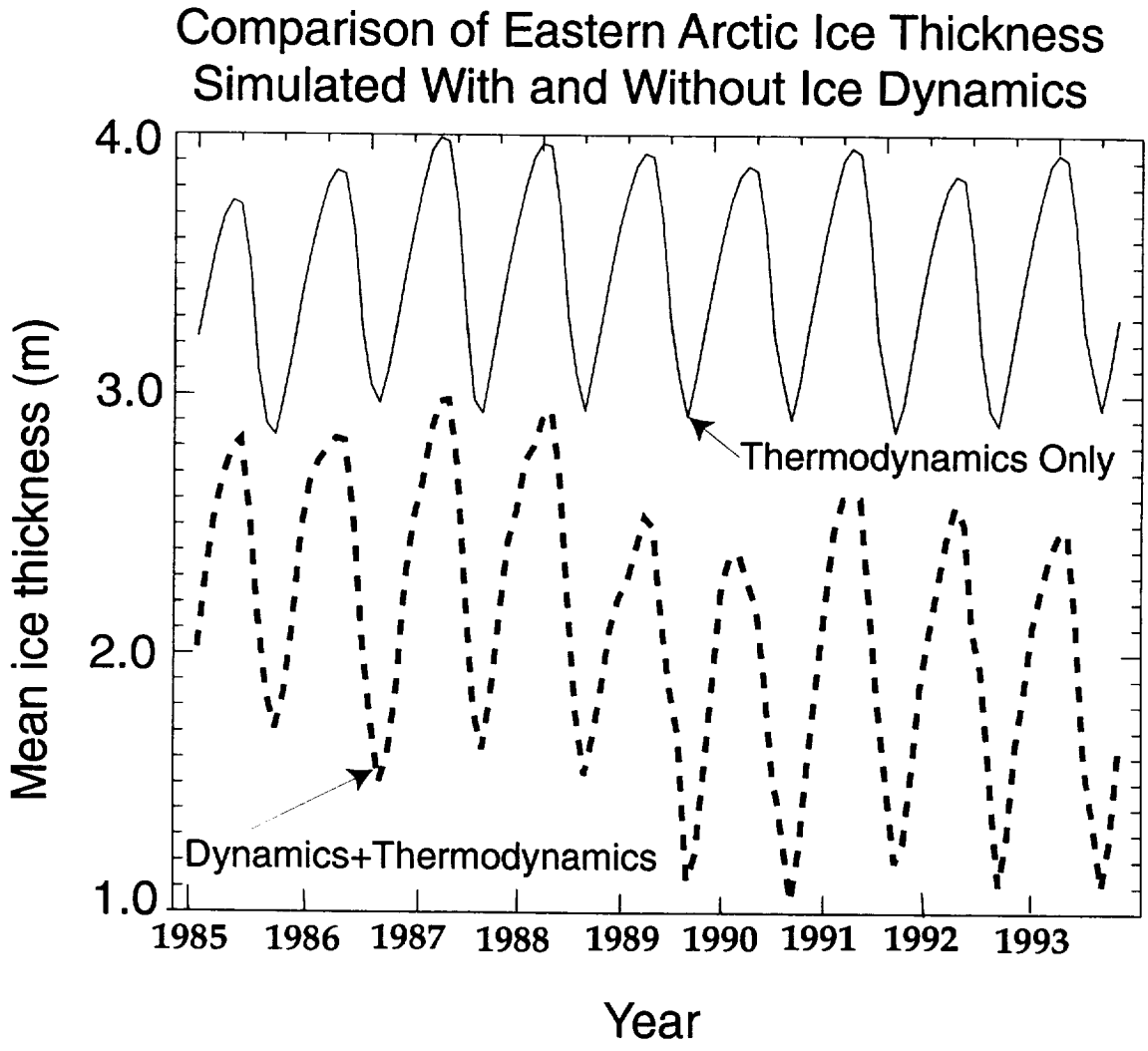

Figure 9. Modeled ice thickness in the eastern Arctic for 1985-1993, illustrating reduced ice thickness since 1989.

A second study used ice motion data to consider the larger-scale effects of changes in atmospheric circulation (Maslanik et al., 1997b). In particular, we considered (a) how the effects of persistence in circulation indices might affect the interpretation of climate signals; and (b) how such persistence affects basin-scale ice transport. The impetus for this work was the fact that the available Arctic buoy observations and satellite data have been acquired during a period of abnormal atmospheric pressure patterns (e.g., a persistent positive NAO and reduced central Arctic SLP). Thirteen of the 17 years of available satellite coverage from 1979-1995 were years with a positive NAO index. Since the early 1960's, the NAO has been increasingly positive (Hurrell and Van Loon, 1997). From 1920 to 1995, six of the 8 years with the largest positive NAO index occurred after 1988, with the period from 1989-1995 exhibiting the strongest and most persistent positive NAO cycle during the 120-year record (Hurrell and Van Loon, 1997; Fig. 5). In addition to the lower SLP near Iceland (e.g., the northern element of the positive NAO mode), SLP in the central Arctic has been below normal in recent years (Walsh et al., 1996), with a substantial increase in cyclonic activity (Serreze et al., 1996). Since nearly all of the satellite and buoy data used to study sea ice conditions have been collected from 1979 onward, the mean fields from these data are likely biased in favor of the recent positive NAO cycle, and thus are not necessarily a reliable map of "typical" Arctic ice transport patterns.

The main results of this investigation are as follows:

- SLP patterns in recent years suggest a central Arctic "extension" of the lower North Atlantic SLP associated with positive NAO years;
- Negative NAO years appear associated with a strengthened Beaufort Gyre, while positive NAO years favor a weaker gyre and greater northward ice transport from the eastern Arctic (East Siberian, Laptev, and Kara seas) into the Transpolar Drift Stream (TDS);
- The recent positive NAO years are characterized by reduced ice extent in the Eastern Arctic, somewhat heavier ice in the Beaufort Sea and Canadian Arctic, and greater ice export through Fram Strait;
- Simulations suggest that the ice cover may be thinner in the Arctic Basin in positive NAO years, and substantially so in the eastern Arctic. This difference depends on ice transport;, and is accentuated for those positive NAO years with the Arctic Basin extension of reduced SLP;
- The NCAR CSM equilibrium simulations yield a strongly anti-cyclonic Arctic mean SLP pattern and sea ice transport. CSM may favor, and perhaps be "locked" into, a strongly-negative NAO pattern - perhaps related in part to CSM's overestimate of ice cover in the North Atlantic;
- Accurate coupled simulations of interannual variability in ice cover thus depends on a model's ability to predict relatively subtle changes in SLP and the resulting interactions among ice dynamics and thermodynamics.

Our comparisons of observed and modeled ice conditions show that the nature of the ice pack (for example, multiyear ice fraction) and the mean transport patterns for mostly-positive NAO years and mostly-negative NAO years are consistent with the mean atmospheric circulation differences between positive and negative NAO events. Ice transport (area) estimated from the remotely-sensed ice motions show that the influx into the Transpolar Drift Stream (and thus the ice advected into the North Atlantic) has a different source region depending on atmospheric circulation regime (figure 10).

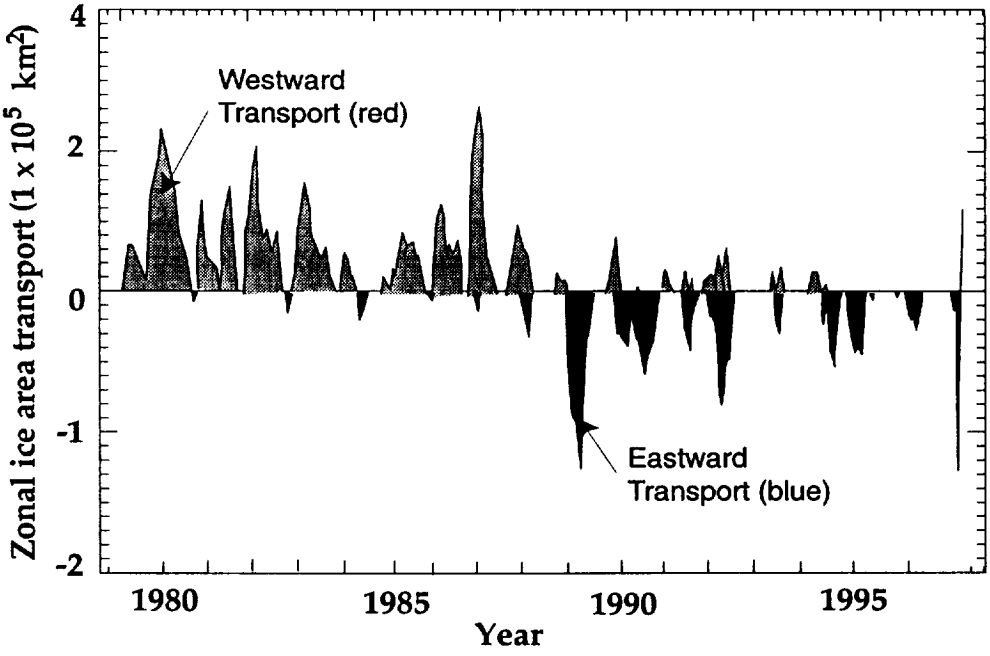

Figure 10. Ice areal transport across the 180° W longitude line from 72° N to 84° N. Positive (light gray) indicates westward transport. Negative (dark gray) indicates eastward transport.

2.4.2 Implications for Climate Change Simulations

We extended the modeling and observational work to investigate how the ability of models to simulation of large-scale transport might affect the realism of climate-change simulations (Maslanik and Dunn, 1997). Sea ice conditions for 1985-1993 were simulated using our 2-D ice model. Interannual differences in ice extent were dominated by ice transport. We found that different transport regimes affected the response of the simulated ice pack to climate perturbations applied to the 2-D model. For example, Figure 11 illustrates the interannual variability in ice extent using a control run with NCEP forcings, and with two different ranges of a "warmer climate"

scenario. The interesting feature of this plot is that, while the model is correct in reproducing the minimum ice extent in 1990 under control conditions, the year with the maximum reduction in ice extent changes when the climate-change scenarios are applied. When we examined ice transport in more detail for this year compared to 1990, we concluded that the reason for this change is that 1986 was a year where transport patterns favored southward advection of the ice pack, while 1990 favored northward transport. As a result, in 1986 more ice was transported to locations where the ice the effects of the climate perturbations were most pronounced. In contrast, in 1990 advection tended to keep ice at high latitudes, so that the summer 1990 ice extent was relatively unaffected by the warmer-climate scenario.

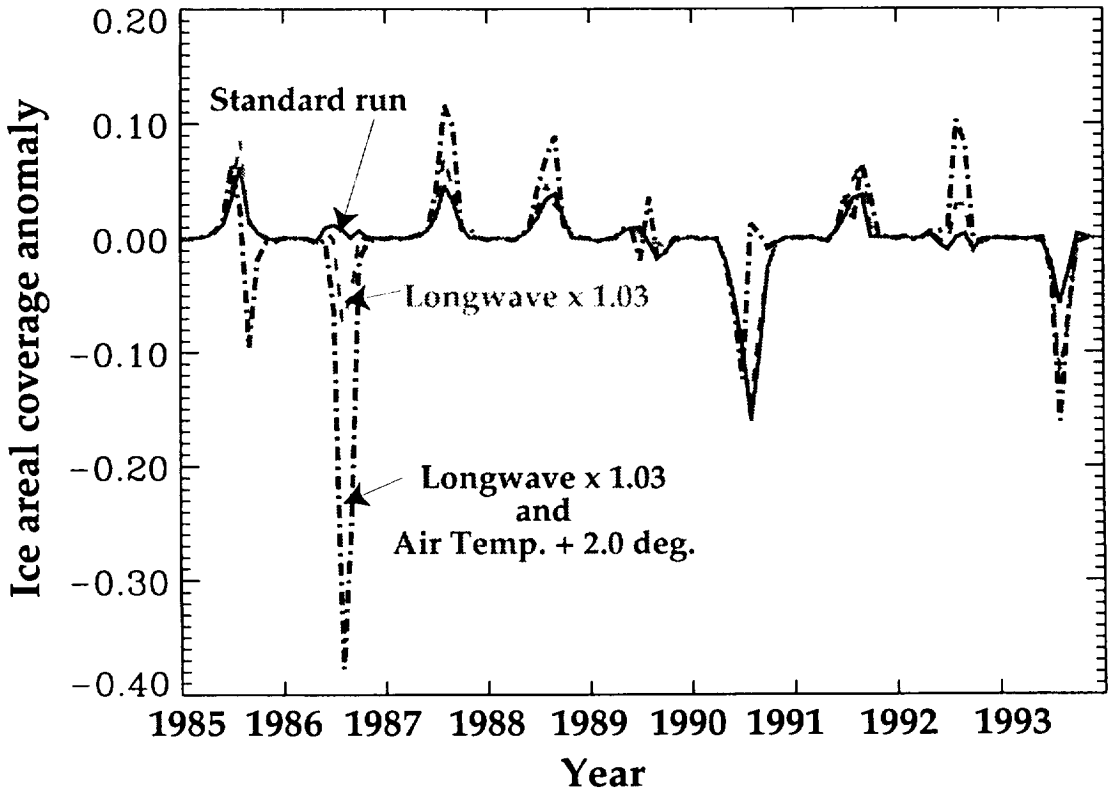

Figure 11. Simulated interannual variability in Arctic ice extent using standard NCEP forcings and NCEP forcings modified to include global warming scenarios.

GCM simulations using the NCAR GENESIS model further illustrated the importance of ice transport in affecting how the ice pack responds to global warming scenarios. Experiments using GENESIS with and without ice transport suggests that much of the difference in the response of the ice pack

in these two runs was due to the effects of ice transport in positioning the ice pack spatially and in affecting the thickness of the pack across the Arctic.

2.5 *Applications of Remotely-Sensed Ice Motion Data for Model Evaluation*

2.5.1 NCAR CSM Evaluation

The satellite-derived motion fields and the motions blended with buoy data were used in several model evaluation efforts ranging from testing the effects of ice rheology to verifying the performance of the National Center for Atmospheric Research Climate System Model (NCAR CSM). SSM/I motion fields for the Southern Ocean such as those shown in Figure 5 were used to calculate ice mass flux for comparison to the CSM estimates. Simulated ice thicknesses supplied by J. Weatherly at NCAR were combined with the SSM/I ice velocities to estimate meridional and zonal ice transport (Weatherly et al., 1998). The transport estimates were then compared to transport simulated by CSM. Based on these comparisons, NCAR investigators concluded that CSM was substantially overestimating northward ice transport, which resulted in an over-production of Antarctic Deep Water due to new ice formation in the overly-divergent ice pack. The problem was later found to be due to a coding error. In this case, the passive microwave-derived motion fields provided the only means of testing the model against observations.

Another apparent shortcoming of the ice transport patterns in the current CSM is a tendency to generate a dominant anticyclonic gyre covering nearly the entire Arctic Ocean. This differs from the observed pattern seen in mean fields from buoy data and our motion products. However, as noted in the previous section, the buoy and remotely-sensed data cover a period when the atmospheric circulation is in a persistent positive-NAO-type pattern (Maslanik et al., 1997b). The negative NAO pattern is more similar to the mean CSM simulations. This suggests a variety of interesting research issues, but also points out the potential danger of taking as "truth" the observations from a relatively short, and perhaps unusual, climatic period.

2.5.2 Evaluation of the Effects of Ice Rheology in 2-D Ice Models of the Arctic

The blended motion fields were used to intercompare ice models using cavitating fluid, viscous-plastic (VP) and elastic viscous-plastic (EVP) ice rheologies (Arbetter et al., 1998; Arbetter and Meier, 1998). In this case, the motion fields provided more spatial detail than is available from drifting buoy data, and allowed assessment of rheology differences in areas where drifting buoys are typically scarce. The VP and EVP results differed least from the observations overall, although differences could be large on individual days. In general, the models tend to overestimate drift speed. Such comparisons suggest that the gridded motion fields will be useful for refining

model parameters, since nearly all such models are run using tuning parameters estimated using relatively few comparisons to buoys.

A small study was also undertaken to test the effects of temporal sampling on estimates of ice divergence (Fowler et al., 1996). AVHRR data sampled over 1 through 7 days were used to calculate open-water production by summing production using daily sampling over the 7-day period, 2-day sampling, etc. Our results showed that open-water production (and thus new ice growth) was underestimated substantially using the 7-day sampling that was originally planned for the RADARSAT Geophysical Processing System. Open water production is considerably undersampled even at 3-day sampling intervals. This suggests that ice motion data should be acquired at the maximum time resolution that is consistent with the spatial resolution of the data. As noted in the discussion of data assimilation, this study also points out the need to avoid smoothing the deformation of the ice pack over time, such as might occur if 3-day sampled ice motions are used in an assimilation without regard to deformation occuring on finer time scales.

3.0 Conclusions

We believe that this project has yielded significant advances in the preparation and application of ice motion products for climate studies. A number of possibilities exist for extending this work. These include more studies taking advantage of the relatively fine-resolution AVHRR motions now being finalized as part of the Polar Pathfinder effort, a need for much additional research in the area of data assimilation, and assessment of the likely improvements in ice motion data to be provided by the Advanced Microwave Scanning Radiometer (AMSR).

4.0 References and Supported Publications/Manuscripts (Indicated by "*")

Agnew, T.A., H. Le and T. Hirose, 1997. Estimation of large-scale sea ice motion from SSM/I 85 GHz imagery. *Annals of Glaciol.*, 25, 305-311.

*Arbetter, T.E. and W.N. Meier, 1998. Comparison of daily satellite-derived Arctic ice motion with model results. *J. Geophys. Res.* (submitted).

*Arbetter, T.E., J.A. Curry, and J.A. Maslanik, 1998. Effects of rheology and ice thickness distribution in a dynamic-thermodynamic sea ice model, *J. Phys. Oceanogr.* (accepted).

*Brasket, A, J. Curry, and J. Maslanik, 1997. Sea-ice variability in the Greenland and Labrador seas and their interaction with the North Atlantic Oscillation. Conference on Polar Processes and Global Climate, ACSYS, WCRP, Orcas Island, WA, USA, 27-29.

Emery, W.J., C.W. Fowler, and J.A. Maslanik, 1997: Satellite derived Arctic and Antarctic Sea Ice Motions: 1988 - 1994. *Geophys. Res. Lett.*, 24, 8, 897-900.

*Emery, W.J., C.W. Fowler, J.A. Maslanik, 1997: Satellite derived Arctic and Antarctic Sea Ice Motions: 1988 - 1994. *Geophys. Res. Lett.*, 24, 8, 897-900.

*Fowler, C.W., W.J. Emery, and J.A. Maslanik, 1996. The consequences of 7-day sampling for ice motion and derived fields. White paper submitted to the RADARSAT Geophysical Processing System Working Group, 17 pgs.

*Heinrichs, J., J.A. Maslanik, and K. Steffen, 1998. The seasonal cycle of sea ice in the Beaufort Sea: A comparison of model output and ERS-1 SAR data using a forward simulation approach. *J. Geophys. Res.* (accepted).

Hurrell, J.W. and H. Van Loon, 1997: Decadal variations in climate associated with the North Atlantic Oscillation. *Climatic Change*, 36, 301-326.

Liu, A.K., D.J. Cavalieri, and C.Y. Peng, 1998. Sea ice drift from wavelet analysis of DMSP SSM/I data, *Geophys. Res. Lett.*, (submitted).

*Maslanik, J.A. and J. Dunn, 1998. On the role of sea ice transport in modifying Arctic responses to global climate change. *Annals of Glaciol.*, 25, 102-106.

*Maslanik, J., C. Fowler, J. Key, T. Scambos, T.Hutchinson, and W. Emery, 1998. AVHRR-based Polar Pathfinder products for modelingapplications. *Annals of Glaciol.*, 25, 388-392.

*Maslanik, J.A., 1998. Combining remote sensing and geophysical modeling to monitor and predict polar sea ice mass and transport. White paper submitted in response to NASA request for planning documents. 5 pgs.

*Maslanik, J., A. Lynch, and M. Serreze, 1997. Modeling of Arctic sea ice anomalies - implications for simulating the sea ice response to global warming, Conference on Polar Processes and Global Climate, ACSYS, WCRP, Orcas Island, WA, USA,153-155.

*Maslanik, J., C. Fowler, W. Emery, and J. Weatherly, 1997. On the interannul variability of Arctic sea ice transport: relationship to atmospheric circulation models and significance for GCM assessments, Conference on Polar Processes and Global Climate, ACSYS, WCRP, Orcas Island, WA, USA, 156-158 (also in preparation for journal submission).

*Maslanik, J.A., M.C. Serreze, and R.G. Barry, 1996. Recent decreases in Arctic summer ice cover and linkages to atmospheric circulation anomalies, *Geophys. Res. Lett.*, 23, 13, 1677-1680.

*Meier, W.N. and J.A. Maslanik, 1998. Error analysis and assimilation of remotely-sensed ice velocities in an Arctic Basin sea ice model. (in preparation).

*Meier, W.N., J.A. Maslanik, J.R. Key, and C.W. W. Fowler, 1997. Multiparameter AVHRR-derived products for Arctic climate studies, *Earth Interactions*, Vol. 1.

Rosenfeld, A. and A.C. Kak, 1982. Digital Picture Processing, vol. 2, 2nd ed., New York: Academic Press.

Serreze, M.C., J.A. Maslanik, J.R. Key, R.F. Kokaly, and D.A. Robinson, 1995. Diagnosis of the record minimum in Arctic sea ice area during 1990 and associated snow cover extremes. *Geophys. Res. Lett.*, 22, 16, 2183-2186.

Walsh, J.E., W.L. Chapman, and T.L. Shy, 1996. Recent decreases of sea level pressure in the central Arctic. *J. Climate*, 9, 480-486.

*Weatherly, J.W., B.P. Briegleb, W.G. Large, and J.A. Maslanik, 1998. Sea ice and polar climate in the NCAR CSM, *J. Climate* , 11, 6, 1472-1486.

Wu, Q.X., 1995. "A Correlation-Relaxation-Labeling Framework for Computing Optical Flow -- Template Matching from a New Perspective", *IEEE Trans. Pattern Analysis and Machine Intelligence*, vol. 17, no. 8, pp. 843-853.